ACS MATERIALS Au
AN OPEN ACCESS JOURNAL OF THE AMERICAN CHEMICAL SOCIETY

pubs.acs.org/materialsau
Article

Biocomposite Macrospheres Based on Strontium-Bioactive Glass for Application as Bone Fillers

Ivone Regina de Oliveira,* Isabela dos Santos Gonçalves, Kennedy Wallace dos Santos, Maria Carmo Lança, Tânia Vieira, Jorge Carvalho Silva, Ibrahim Fatih Cengiz, Rui Luís Reis, Joaquim Miguel Oliveira, and João Paulo Miranda Ribeiro Borges

Cite This: ACS Mater. Au 2023, 3, 646−658
Read Online
ACCESS | Metrics & More | Article Recommendations

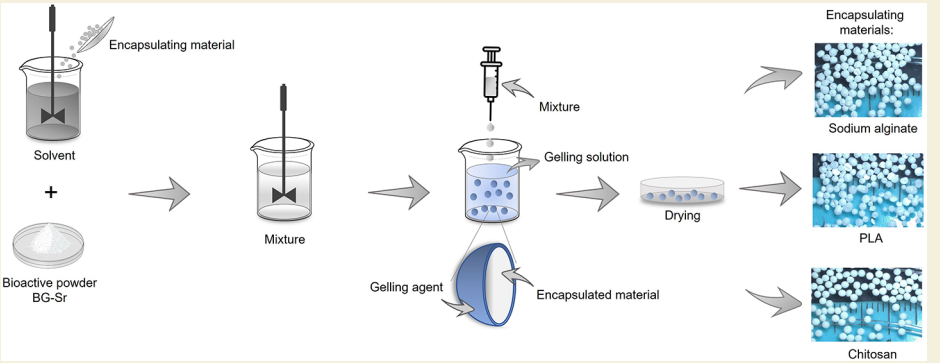

ABSTRACT: Traditional bioactive glass powders are typically composed of irregular particles that can be packed into dense configurations presenting low interconnectivity, which can limit bone ingrowth. The use of novel biocomposite sphere formulations comprising bioactive factors as bone fillers are most advantageous, as it simultaneously allows for packing the particles in a 3-dimensional manner to achieve an adequate interconnected porosity, enhanced biological performance, and ultimately a superior new bone formation. In this work, we develop and characterize novel biocomposite macrospheres of Sr-bioactive glass using sodium alginate, polylactic acid (PLA), and chitosan (CH) as encapsulating materials for finding applications as bone fillers. The biocomposite macrospheres that were obtained using PLA have a larger size distribution and higher porosity and an interconnectivity of 99.7%. Loose apatite particles were observed on the surface of macrospheres prepared with alginate and CH by means of soaking into a simulated body fluid (SBF) for 7 days. A dense apatite layer was formed on the biocomposite macrospheres' surface produced with PLA, which served to protect PLA from degradation. *In vitro* investigations demonstrated that biocomposite macrospheres had minimal cytotoxic effects on a human osteosarcoma cell line (SaOS-2 cells). However, the accelerated degradation of PLA due to the degradation of bioactive glass may account for the observed decrease in SaOS-2 cells viability. Among the biocomposite macrospheres, those composed of PLA exhibited the most promising characteristics for their potential use as fillers in bone tissue repair applications.

KEYWORDS: *bioactive glass, strontium, macrospheres, encapsulation, bone defects*

1. INTRODUCTION

Annually, millions of people suffer from defects in bone tissues, resulting from congenital malformations, tumors, or fractures with poor prognosis, fatally culminating in cases of pseudoarthrosis and osteomyelitis.[1] The treatment of these types of pathologies occurs through a surgical procedure aimed at the mechanical removal of the affected tissues, followed by the application of bone grafts alone or in conjunction with a gradual bone transport procedure using external fixators. This procedure is aimed at restoring the shape and the function of the injured tissue through a bone reconstruction process.[1]

The application of xenogenous bone grafts (of animal origin) has been indicated as an alternative to autogenous and allogeneic grafts (of human origin). However, all these grafts of biological animal origin still can present risks of infection, rejection, and long recovery periods. Moreover, xenogenous

Received: May 31, 2023
Revised: July 18, 2023
Accepted: July 20, 2023
Published: August 1, 2023

https://doi.org/10.1021/acsmaterialsau.3c00048
ACS Mater. Au 2023, 3, 646−658

bone grafts typically have less bone formation ability as compared to autogenous grafts.[2] In addition to the aforementioned limitations, clinical reasons related to extensive bone defects, where filling using grafts without three-dimensional structure is inevitable, justify the development and applicability of synthetic (alloplastic) biomaterials for bone grafts.[3,4]

Worldwide, it is estimated that around 2.2 million procedures involve the use of bone grafts, with a demand growing by alloplastic grafts replacing autogenous and allogeneic grafts. Sales of bone grafts and substitutes are expected to reach US$ 4.44 billion by the end of 2028. The types of applications that use bone grafts can be divided into the following large areas: long bone reconstructive surgery, foot and heel surgery, craniofacial surgery, joint surgery, dentistry (implant dentistry), and spine surgery.[5]

Several companies, such as Botiss Medical AG, Straumann Holding AG, Baumer, Geistlich and Critéria, sell grafts in the form of granules, membranes, pastes or scaffolds.[6] Some of its products available on the market correspond to mineralized bovine bone (composed of collagenous proteins and hydroxyapatite mineral), synthetic biphasic ceramic biomaterials (hydroxyapatite and calcium β-triphosphate), deproteinized bovine bone (inorganic matrix of spongy medullary bovine bone), demineralized bovine bone matrix (lyophilized porous organic matrix extracted from bovine cortical bone), and mineralized porcine bone (composed of collagen).[5,6]

Considering only bioactive glass bone grafts, most of the products are available in pasty form, such as BioSphere Putty, a composite consisting of spherical particles of Bioglass 45S5 with a resorbable phospholipid matrix (Synergy Biomedical); Bonalive Putty, composite made of bioactive glass S53P4 with a mixture of polyethylene glycols (PEGs) and glycerol (Bonalive); and Activioss Injectable Putty, composite made of Bioglass 45S5 and unidentified polymer (Noraker[5,6]).

The use of bioactive glasses (BG) as alloplastic grafts has been reported by a wide range of scientific studies, with recognized advantages in terms of biocompatibility, osteoinduction, and osteoconduction.[7,8] In addition, they possess improved bioactivity and degradation properties as compared to hydroxyapatite and β-tricalcium phosphate.[9] This results from their remarkable capability to chemically bond with bone tissues due to the formation of an apatite-like layer on its surface upon exposure to physiological fluids. Thus, they have become very promising materials as bone graft material.

A product for bone grafting (BioSphere Putty) has been developed by the company Synergy Biomedical using spherical particles and an optimized size range of bioactive glass.[10] That material, when implanted in a critically sized femoral defect, showed bone growing through the entire defect in a shorter time as compared with conventional bioactive glass products with irregular particles. In addition, the bone healing properties of BG were substantially improved.[10] Interestingly, the spherical shape facilitated the arrangement of particles in a three-dimensional (3D) structure, thus ensuring 100% interconnected porosity. This enhanced porosity eliminates the presence of small pores or blocked-off channels, thereby promoting improved bone growth across the entire implant area.[10]

In addition to bioactive ceramics, various materials, including natural or synthetic polymers and their composites, have been fabricated into microspheres for bone-defect repair.[4] Spheres can offer a significant advantage as compared to prefabricated scaffolds as they possess the capability to release active substances and effectively fill irregular and complex bone defects of varying sizes and shapes. The space among the spheres facilitates internal bone growth and enables proper vascularization, ensuring optimal conditions for successful bone regeneration.[4,9] In order to address various requirements of bone tissue engineering, porous, core−shell, and multi-compartmental microspheres have been developed.[4]

By means of microencapsulation techniques, substances in solid, liquid, or gas are surrounded with a coating material, typically a polymeric agent, allowing the controlled release of several bioactive compounds.[11,12] Spheres based on bioactive ceramics have been developed using polylactic acid (PLA), polyglycolic acid (PGA), gelatin, alginate, and chitosan (CH) due to their biocompatibility and complete bioresorbability.[11,13−16] Improvement in the properties of bioceramic microspheres as slow degradation rates and high brittleness is obtained for creating composite microspheres.[4]

Strontium (Sr) has also been studied as a bioactive element to induce bone tissue regeneration.[17−19] This element shares chemical properties similar to those of calcium ions, which are fundamental components of bone tissue, thereby exhibiting comparable physiological and biological characteristics. Over the past decade, there has been growing interest in the properties of Sr, primarily due to the development of strontium ranelate, a medication used for treating osteoporosis, predominantly in postmenopausal women. Strontium ranelate stands apart from other drugs, as it exerts a novel and distinct effect on osteoporosis treatment by enhancing osteogenesis while simultaneously inhibiting osteoclastogenesis.[20] Sr accumulates to a high degree in bone owing to its bone-seeking behavior but at high concentrations interferes with normal bone development.[17,19]

Therefore, according to the literature, BG incorporated with Sr has gained considerable attention in the recent past for various orthopedic applications joining the effect of surface bioactivity of BG with the promotion of bone growth due to Sr-controlled release. A previous study[21] showed that BG compositions containing Sr resulted in a superior cell viability at higher extract concentrations, and superior amorphous calcium phosphate formation as compared with BG without Sr. Furthermore, the use of BG with a spherical shape and bimodal size range tends to maximize its bone healing potential.

In this work, we developed different biocomposite macrosphere formulations based on strontium-bioactive glass (BG-Sr) for application as bone fillers. We hypothesize that the type of encapsulating materials, in particular sodium alginate, polylactic acid (PLA), or chitosan (CH), can influence the macrosphere characteristics such as bioactivity and absorbability. The physicochemical properties of BG spheres were comprehensively evaluated using various techniques, including size distribution analysis, X-ray diffraction analysis, Fourier transform infrared spectroscopy, microcomputed tomography analysis, specific surface area measurement, theoretical density determination, and bioactivity testing. Additionally, an in vitro cytotoxicity screening of BG spheres was conducted using SaOS-2 cells, a human osteosarcoma cell line.

2. MATERIALS AND METHODS

2.1. Macrospheres' Production

Macrospheres of strontium-bioactive glass (BG-Sr) were produced by microencapsulation techniques using sodium alginate, poly(lactic

https://doi.org/10.1021/acsmaterialsau.3c00048
ACS Mater. Au 2023, 3, 646−658

acid) (PLA), or chitosan (CH) encapsulating materials. The BG-Sr used has the nominal composition (58 SiO_2, 28 CaO, 5 SrO, 9 P_2O_5 in wt %) and it was synthesized as previously described elsewhere.[21]

2.1.1. Alginate/BG-Sr Macrospheres. The production of Alginate/BG macrospheres involved the extrusion method, which entailed combining the material to be encapsulated with a solution of an encapsulating material, such as sodium alginate. This mixture was thoroughly homogenized and subsequently extruded into a gelling solution, resulting in the formation of macrospheres.[22−25] Alginate can exchange ions with divalent ions to form a stable "egg-box" hydrogel owing to the unique ionotropic-gelation effect.[4] The methodology used followed the series of steps reported elsewhere.[9]

BG-Sr powder was added to water (3.125 g/40 mL) and stirred for 30 min to form a slurry. Alginic acid sodium salt (3.0 g, $NaC_6H_7O_6$, Biochemica) was then dissolved in 100 mL of water to form the alginate solution with a concentration of 3% (w/v) and stirred for 30 min at 50 °C. The alginate solution was added to the slurry and stirred for 1 h at 50 °C and ultrasonicated for 5 min to form homogeneous mixtures. The mixture (BG:alginate 1:1) was kept under agitation and heating (50 °C) while being extruded dropwise with a syringe connected to an infusion pump (1 mL/min, Kdscientific, USA) into 300 mL of gelling solution 0.1 M calcium chloride dihydrate ($CaCl_2{\cdot}2H_2O$, 99%, Honeywell Fluka) while maintaining low stirring. Following a 30 min incubation period in the gelling solution, the macrospheres underwent a series of subsequent steps. These included washing in distilled water (300 mL, three times) for 30 min and ethanol (100 mL) for 15 min, filtration, a 15 min drying phase under hot air, followed by 24 h of drying in an oven at 60 °C. Finally, the macrospheres were calcined at 630 °C for 8 h, with a heating rate of 1 °C per minute. These procedures resulted in the production of exclusively bioglass spheres, commonly referred to as MBG-Sr.

2.1.2. PLA/BG-Sr Macrospheres. BG-Sr was also encapsulated into the polymer PLA matrix-producing polymer/ceramic composite macrospheres. This procedure is based on a solid-in-oil-in-water (s/o/w) emulsion solvent removal method.[14]

PLA (2.1 g, LX 175, Total Carbion) was dissolved in 15 mL of dichloromethane (>99.9%, Sigma-Aldrich) with magnetic stirring. The BG-Sr powder (2.1 g) was mixed with the PLA solution (BG:PLA 1:1) via sonication for 15 min. The mixture was then added drop by drop with a syringe connected to an infusion pump (1 mL/min, Kdscientific, USA) into 400 mL of poly(vinyl alcohol) (PVA) (95% hydrolyzed, Acros Organics) solution vigorously stirred, previously prepared at a concentration of 0.5% with magnetic stirring at 90 °C for 2 h. The solution containing macrospheres (MPLA/BG-Sr) was stirred for 4 h at room temperature to remove the solvent to improve their biocompatibility. After, the macrospheres were washed in 200 mL of distilled water (three times), filtered, dried in an oven at 60 °C for 24 h, and stored in a desiccator.

2.1.3. CH/BG-Sr Macrospheres. BG were last encapsulated into the biodegradable polymer CH matrix producing polymer/ceramic composite macrospheres. This procedure is based on the ionotropic gelation technique.[16,26] CH is a nature-derived cationic polymer that can react with polyanions to prepare microspheres with a gel network.[4]

The CH solution was prepared by dissolving 2.5 g of cationic polymer of marine origin (80% deacetylation, Chitopharm S, Cognis) in 100 mL of acetic acid solution (99.7%, Panreac) previously prepared at a concentration of 5%. This mixture was gently stirred at room temperature to avoid air bubbles and obtain a homogeneous viscous solution. The BG-Sr powder (2.5 g) was added to the CH solution (BG:CH 1:1) and mixed for 20 min. The mixture was extruded dropwise with a syringe connected to an infusion pump (1 mL/min, Kdscientific, USA) into the gelling solution of 12% sodium hydroxide (100%, Eka). After 24 h incubation in the gelling solution, the macrospheres (MCH/BG-Sr) were washed in 1 L of distilled water several times until pH stabilization. Next, they were washed with 300 mL of ethanol for 15 min and left in 300 mL of acetone for 24 h. Finally, macrospheres were filtered, dried under air for 6 h, and in an oven at 60 °C for 24 h.

2.2. Macrospheres' Characterization

2.2.1. Physicochemical Characterization. The size distribution of the macrospheres was determined from images obtained with a magnifying glass (Leica S9i, LAS v4.12) using ImageJ. For each measurement, the size distribution of 200−250 macrospheres was analyzed. The diffraction patterns (XRD) were obtained in the 2θ range from 10° to 90° in continuous scan mode using a PANalytical model Xpert PRO MRD diffractometer operating with CuKα radiation (wavelength 1.540598 Å). Fourier transform infrared spectroscopy (FTIR) spectra were obtained using a Thermo Nicolet 6700 spectrometer operating in attenuated total reflectance (ATR) mode with a 4 cm^{-1} resolution in the 4500−525 cm^{-1} region. The microcomputed tomography (micro-CT) characterizations were performed with a high-resolution desktop micro-CT system, SkyScan 1272 scanner (Bruker Micro-CT, Belgium). Qualitative and quantitative characterization of the shape, and porosity within the gross volume of the particles were performed.[27,28] Also, the particles were put into a transparent holder and scanned to study the packed condition. The image acquisition was performed without a filter; the pixel size was 5 μm, and the source voltage and current were set to 35 kV and 181 μA, respectively. A total of 900 2D X-ray projections with the size of 1092 pixels × 1632 pixels were acquired over a sample rotation range of 360° with a rotation step of 0.4° that took around 35 min per acquisition. The projections were then reconstructed to obtain cross-sectional images with NRecon software (version 1.6.10.2) from Bruker. The 3D models were built from 2D images. The porosity analysis, and interconnectivity[29,30] of the packed spheres were obtained through the analysis done by using the CT Analyzer software (v1.15.4.0) from Bruker as indicated by the manufacturer.

Specific surface area (BET method) analyzer was evaluated using a Nova 2200e Quantachrome Instruments and the theoretical or real density of the spheres, previously dried at 110 °C for 24 h, was evaluated via helium pycnometry technique (Ultrapyc 1200e, V5.04). Composite macrospheres prepared with alginate and CH were crushed in a mortar, and the powder was used in the analysis of XRD and FTIR while PLA-composite was evaluated in discs. Furthermore, bioactivity and cytotoxicity screening were evaluated *in vitro*.

2.2.2. Bioactivity Tests. To evaluate bioactivity, macrospheres of each composition (0.5 g) were immersed in polyethylene containers containing 50 mL of simulated body fluid (Kokubo's SBF) based on ref 31. The containers were constantly agitated at 45 rpm by using an incubator shaker (Optic Ivymen System) at a temperature of 37.5 °C. The immersion was carried out for various durations, including 1, 7, 14, and 21 days. XRD and FTIR tests were used to evaluate the sample surfaces as apatite precipitation after SBF treatments. Briefly, the samples were removed from SBF, washed with water and acetone, and finally dried at room temperature for 3 days. The macrosphere morphological surfaces were studied by scanning electron microscopy (SEM, Tabletop Microscope TM3030Plus, Hitachi). The supernatants were evaluated for pH using a professional bench meter XS. The pH measurements were collected in duplicate and expressed as a mean.

2.2.3. *In Vitro* Studies. For the cytotoxicity assay, SaOS-2 cells (a human osteosarcoma cell line obtained from the American Type Culture Collection, ATCC, USA) were thawed and cultured in a 75 cm^2 flask (Corning Inc.) using McCoy's 5A medium (Sigma-Aldrich, # M4892). The medium was supplemented with 2.2 g/L sodium bicarbonate (Sigma-Aldrich, # S5761), penicillin (100 U/mL), streptomycin (100 μg/mL) (Invitrogen, # 15140122), and 10% fetal bovine serum (FBS) (Invitrogen, #10270106). Once the cells reached confluence, they were counted, resuspended in fresh medium, and plated at a density of 25 000 cells/cm^2 into a polystyrene 96-well plate. The cells were allowed to adhere for 24 h before being exposed to the extract of the evaluated compositions. Throughout the entire cultivation period, the cells were maintained at 37 °C, in a humid atmosphere with 5% CO_2 and 95% atmospheric air.

Prior to use, the macrospheres (0.2 g) were placed in closed glass vials and taken to an oven (P Selecta) for sterilization at 120 °C for a duration of 2 h. The extracts of macrospheres were diluted in culture

https://doi.org/10.1021/acsmaterialsau.3c00048
ACS Mater. Au 2023, 3, 646−658

medium by adding the samples to McCos 5A culture medium at a ratio of 100 mg/mL (sample to medium) according to the International Standard Organization (ISO/EN 10993-5). After incubating at 37 °C for 48 h in a humid atmosphere containing 5% CO_2 and 95% of atmospheric air (CO_2 incubator, Sanyo), the mixtures were filtered with a sterile syringe filter (0.22 μm, 13 mm, Branchia), and the supernatant was collected. Serial dilutions of extracts (50, 25, 12.5, and 6.25 mg/mL) were prepared using McCos 5A medium. The diluted extracts were used in subsequent SaOS-2 cell culture experiments.

Following a 24 h incubation period, the culture medium was aspirated and replaced with 100 μL of extracts. The cells were then incubated for an additional 48 h at 37 °C, in a humid atmosphere with 5% CO_2 and 95% atmospheric air using a CO_2 incubator (Sanyo). Culture medium without the addition of extracts was used as a negative control (C^-) and 10 μL of 10% dimethyl sulfoxide (DMSO) was added to the medium and used as a positive control (C^+).

Viability/cytotoxicity was quantitatively assessed by a colorimetric test that uses a substance that is reduced by live cells. Resazurin is a very low cytotoxic nonfluorescent blue dye that can be used as an indicator of cell viability. Resazurin is reduced by metabolically active cells to resorufin, a pink fluorescent compound. The media was aspirated and 100 μL of medium with resazurin (resazurin sodium salt, $C_{12}H_6NNaO_4$, Alfa Aesar) was placed: 50% of complete culture medium and 50% of a solution of resazurin at 0.04 mg/mL in PBS (phosphate buffered saline). After 3 h of incubation at 37 °C, in a humid atmosphere containing 5% CO_2 and 95% of atmospheric air (CO_2 incubator, Sanyo) the absorbance of each well (570 and 600 nm, ELx800, Biotek Instruments) was read. The result corresponding to each tested condition was expressed by the relative viability, the ratio between the viability of the cells in the condition that was tested and the viability of the cells in the negative control condition. In addition, PLA/BG macrospheres treated in SBF, macrospheres produced using BG after being treated in SBF, and PLA pellets and microspheres produced without BG (MPLA) were also evaluated regarding their cell viability). The experiments were made in quadruplicate.

2.3. Statistical Analysis

Data were reported as means and standard deviation (SD). The differences among the groups were determined using a one-way ANOVA with a post hoc test (Tukey). Statistical significance was set at $p < 0.05$.

3. RESULTS AND DISCUSSION

3.1. BG-Sr Macrospheres Produced by Different Encapsulating Materials

The size distribution of BG 58S (MBG-Sr) and the composite with PLA (MPLA/BG-Sr) or CH (MCH/BG-Sr) is shown in the histogram (Figure 1). Macrospheres (diameter >1 mm) with a more uniform size distribution (1.2−1.6 mm) were obtained using alginate and CH. On the other hand, macrospheres with larger size distribution were obtained using PLA (0.8−2 mm), which may affect their release rate of encapsulated factors and their injectability.[4] Commercially, the size of BG in the form of grains varies with the function of the application. BG grains in the 1−2 mm size range are indicated for orthopedic, trauma, and septic surgery. Microspheres (nHAp/PLGA) with approximately 250 μm exhibited bone-repair capacity.[4] On the other hand, nanosized sphere sizes result in inadequate space for tissue and vascular ingrowth and for carrying bone forming cells.[9,14] In addition, typical45S5 bioactive glass products have irregular particles with a wide range of sizes. On the other hand, new generation of products bring spherical particles with narrow size variation, bimodal increasing the bone formation properties of 45S5.[10]

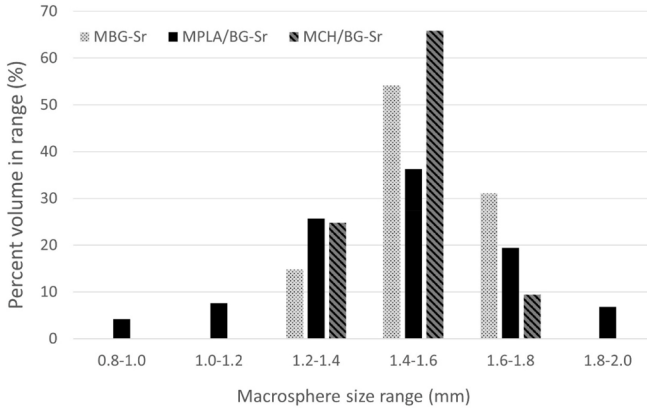

Figure 1. Size distribution histogram of spheres: BG 58S−Sr (MBG-Sr) and a biocomposite with PLA (MPLA/BG-Sr) and chitosan (MCH/BG-Sr).

Macrospheres produced by the method of alginate cross-linking with Ca^{2+} ions possessed irregular shapes with less internal porosity as analyzed by Micro-CT (Figure 2). On the other hand, the solvent removal (PLA) method and ionotropic gelation technique (CH) resulted in a more regular shape and hollow sphere mainly MPLA/BG-Sr.

The bulk analysis of the packed particles revealed a mean porosity of 64.9%, 83.1%, and 71.1% and interconnectivity of 97.3%, 99.7%, and 98.3%, respectively, for MBG-Sr, MPLA/BG-Sr, and MCH/BG-Sr samples (Table 1). These results demonstrated that the developed macrospheres were produced with a desirable architecture allowing the achievement of a desirable interconnectivity when packed.

Spherical particle packing results in 100% interconnected porosity (no small pores or blocked channels) and allows for bone growth across the entire implant area. Due to the spherical shape, the particles can be accurately separated into narrow size ranges. Using specific size ranges can allow a higher degree of control over the dissolution and ion release profile. Small particles are reabsorbed more quickly and generate ions more quickly than larger particles. Larger particles are resorbed more slowly and function as a long-term scaffold for bone formation. Thus, spherical particles can maintain an ideal porosity for bone growth.[10]

It has also been reported that solid ceramic microspheres have higher density as compared to the culture medium, thus producing high shear stresses on cells grown on these microspheres in rotating bioreactors.[14] On the other hand, on hollow bioceramic microspheres the cells experienced very low shear stresses.[14] Furthermore, the macrosphere composites combine the osteoconductivity and bioactivity of bioactive glasses with the ease of polymer processing, which in turn are resorbable but have poor bioactivity.

In this study, the specific surface area (BET method), pore volume, pore diameter, and real density of the macrospheres were investigated (Table 1). A composite with PLA (MPLA/BG-Sr) or CH (MCH/BG-Sr) resulted in macrospheres with lower real density as compared to MBG-Sr due to the low density of polymers.

Figure 3 shows the XRD diffractograms (Figures 3a and b) and FTIR spectra (Figures 3c and d) of the BG 58S−Sr and MBG-Sr produced by the method of alginate cross-linking with Ca^{2+} ions before and after soaking in SBF for different testing times. The presence of peaks indicative of apatite formation

https://doi.org/10.1021/acsmaterialsau.3c00048
ACS Mater. Au 2023, 3, 646−658

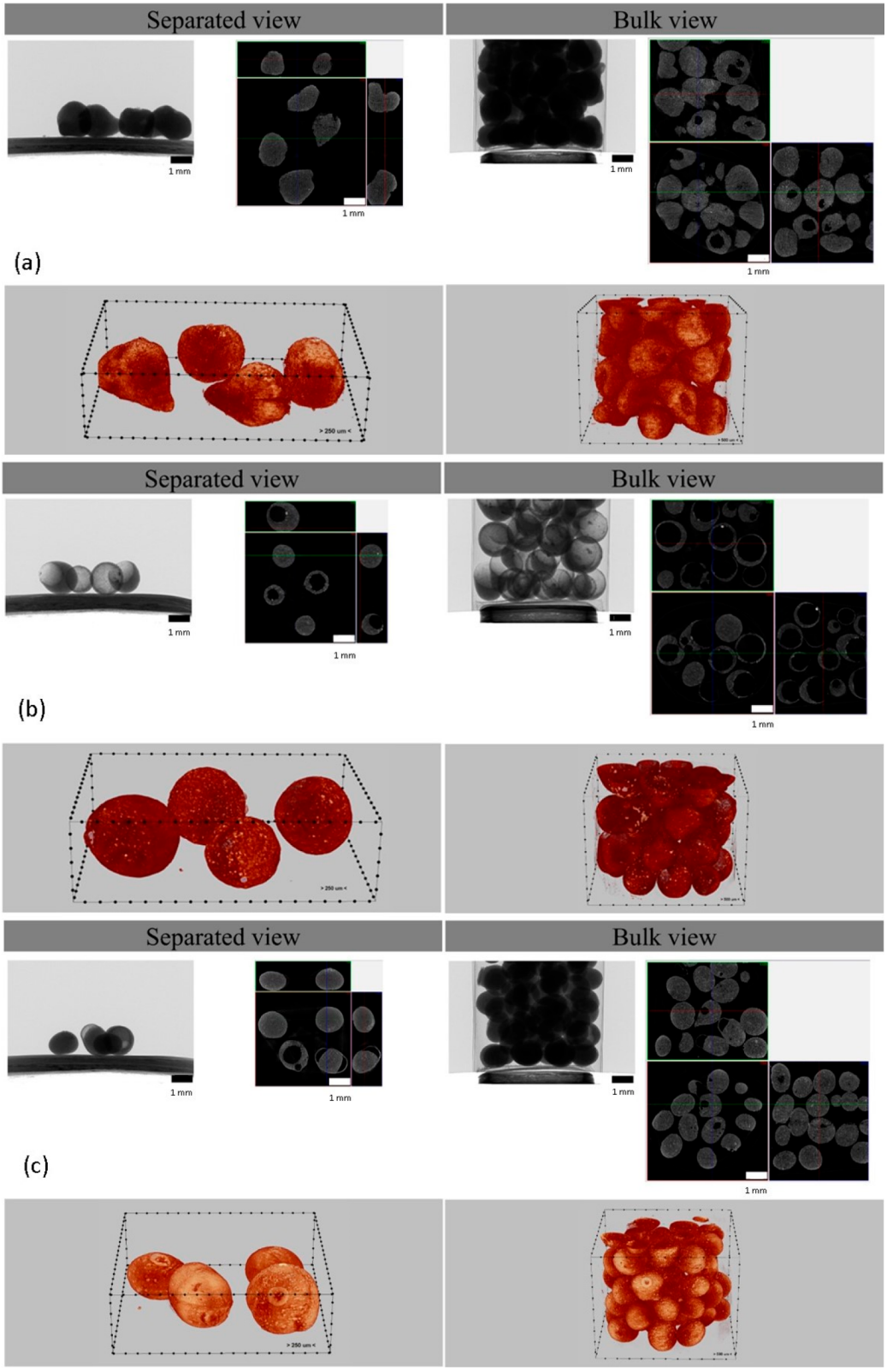

Figure 2. Micro-CT analysis of macrospheres: (a) BG 58S-Sr (MBG-Sr), and the biocomposite with (b) PLA (MPLA/BG-Sr) and (c) chitosan (MCH/BG-Sr).

can be observed in the BG-Sr material used for sphere production. This observation is consistent with the trend of BG prepared with phosphoric acid to form calcium phosphate phases.[21] These peaks become more pronounced upon dissolution of BG in the gelation solution ($CaCl_2$), which is rich in calcium ions. All compositions presented mainly evidence of the formation of crystalline calcium carbonate before and after soaking in SBF for 1, 7, 14, and 21 days.

Prior to immersion in simulated body fluid (SBF), the dominant peak observed in the spectra (1000−1030 cm^{-1})

https://doi.org/10.1021/acsmaterialsau.3c00048
ACS Mater. Au 2023, 3, 646−658

Table 1. Characterization of BG 58S-Sr (MBG-Sr) and Biocomposite with PLA (MPLA/BG-Sr) and Chitosan (MCH/BG-Sr) for Their Properties

Properties	MBG-Sr	MPLA/BG-Sr	MCH/BG-Sr
Overall 3D shape qualitative observation	Irregular shape and not spherical, has a low amount of porosity inside	Sphere with a hole inside	Sphere with or without porosity
Gross volume of the particle (μm^3)	1908 ± 342	1586.9 ± 362	1225 ± 276
Porosity within the gross volume of the particle (%)	3.5 ± 1.7	48.2 ± 18.2	13.6 ± 16
Porosity when packed (%(	64.9 ± 0	83.1 ± 0	71.1 ± 0
Interconnectivity when packed (%(	97.3 ± 0	99.7 ± 0	98.3 ± 0
Specific surface area -BET (m^2/g)	34.0 ± 1.9	23.7 ± 0.6	0
Pore volume (mL/g)	0.139 ± 0	0.094 ± 0	0.002
BJH pore diameter (μm)	0.010 ± 0	0.0079 ± 0	-
Real density (g/cm^3)	2.87 ± 0.03	1.77 ± 0.02	1.53 ± 0.07

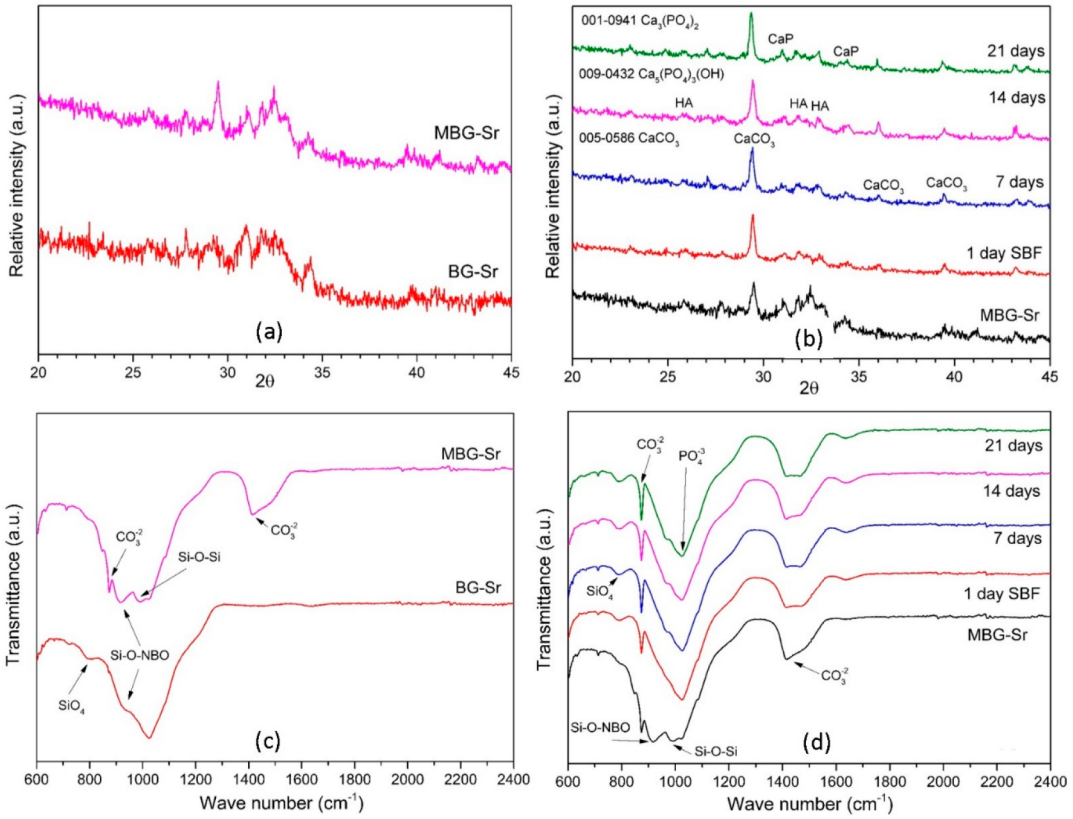

Figure 3. (a, b) XRD patterns and (c, d) FTIR spectra of BG 58S-Sr and macrospheres MBG-Sr produced by the method of alginate cross-linking with Ca^{2+} ions, before and after soaking in SBF for different testing times.

corresponds to the symmetric stretching of the silicon−oxygen−silicon (Si−O−Si) bond, indicating the presence of bridged oxygen.[32] The presence of network modifiers such as calcium and strontium causes the disruption of the continuity of the glassy network due to the breaking of the Si−O−Si bonds leading to the formation of nonbridging oxygen species (Si−O−NBO).[33,34] The band at 800 cm^{-1} is attributed to the deformation vibration of Si−O−Si bridging bonds in the SiO_4 tetrahedrons, which have four oxygen atoms linked to four Si neighbors. The Ca presence is identified due to the presence of a peak at 950 cm^{-1} related to Si−O−Ca bonds containing nonbridging oxygen. The bands observed at 872 and 1460 cm^{-1} can be attributed to the absorption of carbonate, indicating the reactivity of gel-derived glasses with atmospheric CO_2.[9,14,35,36] The vibration band at approximately 1055 cm^{-1} is associated with the vibrational modes of phosphate groups (P−O).[37,38] The samples had an overlapping peak of PO_4^{3-} at the wavenumber of 1030 cm^{-1} and Si−O at the wavenumber of 980 cm^{-1}.[9]

After immersion in the SBF solution, the band characteristic for Si−O bonds at 800 cm^{-1} became more visible. The results validated the presence of a surface layer rich in SiO_2, affirming its formation through the dissolution of the glassy network. Additionally, there was a noticeable increase in the intensity of the PO_4^{3-} peaks at the wavenumber 1030 cm^{-1}, thus suggesting the development of a phase like apatite, which can cause the weakening and finally the disappearance of the bands attributed to Si−O−Si vibration from bioactive glass.[39] Peaks at 1045 and 1090 cm^{-1} are also assigned to the P−O bond although masked by the broad silicate band.[36] XRD analysis before soaking in SBF (Figure 4a) shows that BG-Sr is mostly embedded in the polymer matrix since the intensity of

https://doi.org/10.1021/acsmaterialsau.3c00048
ACS Mater. Au 2023, 3, 646−658

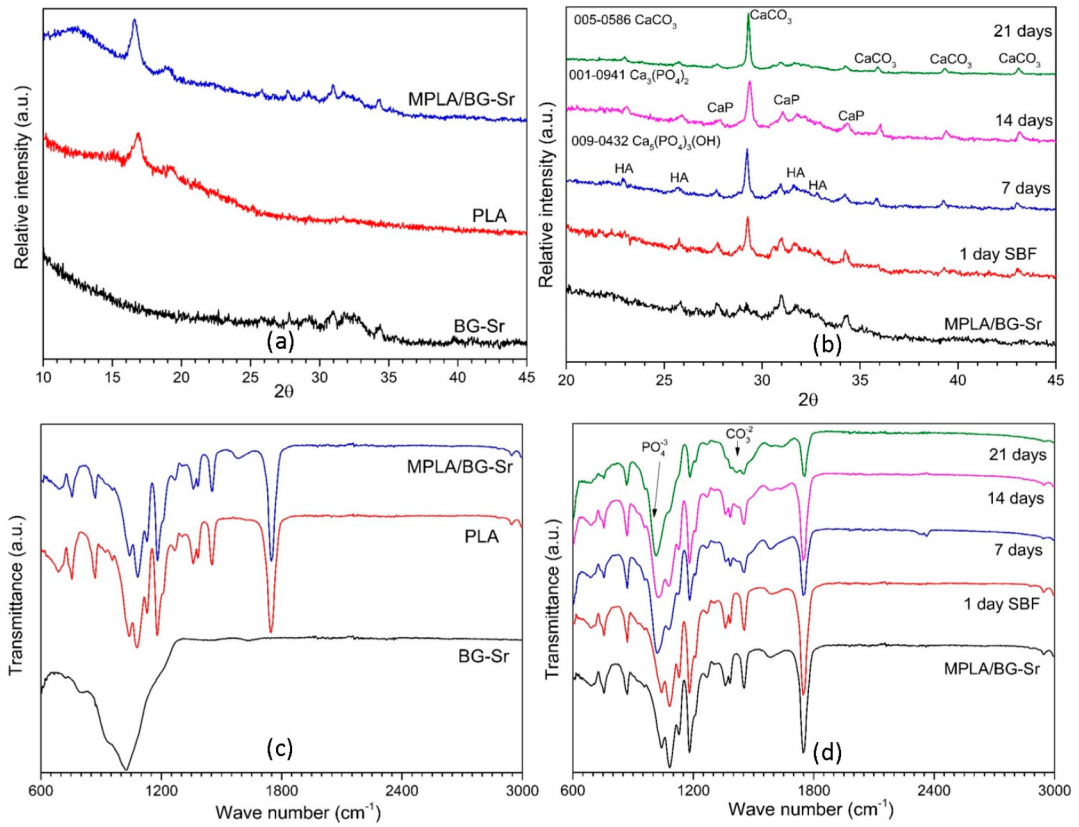

Figure 4. (a, b) XRD patterns and (c, d) FTIR spectra of BG 58S-Sr and PLA, and composite macrospheres (MPLA/BG-Sr) produced by the solvent removal method, before and after soaking in SBF for different testing times.

the characteristic peaks of BG decreases. After soaking in SBF, the spheres MPLA/BG-Sr also present evidence of crystalline calcium carbonate formation (Figure 4b).

Prior to soaking in SBF (Figure 4c), the samples had a spectrum characteristic of PLA. After the SBF treatment (Figure 4d), the intensity of the PO_4^{3-} peaks at the wavenumber 1030 cm^{-1} increased from 7 up to 21 days, thus indicating the formation of the apatite-like phase. The PO_4^{3-} bands at 1046 cm^{-1} in the spectra of the PLA/BG-Sr microspheres immersed in SBF for 14 and 21 days were also assigned to HA and the intensity of the P−O bands increased with incubation time.[14]

XRD analysis before soaking in SBF (Figure 5a) shows that BG-Sr is mostly embedded in the CH matrix since the intensity of the characteristic peaks of BG decreases. After soaking in SBF, the compositions of MCH/BG-Sr present evidence of the formation of amorphous apatite and calcium carbonate phases (Figure 5b).

Prior to soaking in SBF (Figure 5c), the biocomposite macrospheres showed characteristic bands of both CH and bioactive glass. According to the literature, some chemical interactions between the bioactive glass and the CH ensure a good combination between both to form the composite macrospheres.[16]

After soaking in the SBF solution (Figure 5d), the characteristic bands of the composites are modified strongly due to their interfacial reactions with the SBF solution. The spectrum of biocomposite macrospheres shows a well-defined phosphate band at 1039 cm^{-1} after 14 days of soaking, indicating the formation of a phase like apatite. The carbonate bands observed at 874 cm^{-1} are characteristic of a bending vibration. Moreover, the band at 1420 cm^{-1}, attributed to a stretching vibration of the C−O bonds, is also very intense and in agreement with the literature.[16]

3.2. Microstructure and Morphological Characterization

To assess the surface reactivity of the macrospheres, they were immersed in a simulated body fluid (SBF). SEM analysis showed that prior to soaking in SBF, the composite macrospheres were predominantly coated with PLA or CH materials. Figure 6 revealed the morphologies of MBG-Sr, MPLA/BG-Sr, and MCH/BG-Sr, before and after being exposed to SBF for 7 and 14 days. Following immersion in SBF, the formation of a surface layer comprising loosely arranged semispherical apatite particles was observed (Figure 6a). For macrospheres prepared with PLA, a dense apatite layer film with small CaP nodules (apatite clusters) was formed on their surface, as depicted in Figure 6b (MPLA/BG-Sr). MPLA/BG-Sr stands out for its potential to induce the formation of HA on its surfaces, which should stimulate its ability to adhere to bone. On the other hand, the apatite formation was less apparent for macrospheres prepared with CH, as shown in Figure 6c (MCH/BG-Sr). This could be attributed to the presence of CH polymer that may have prevented the calcium ions dissolution, as reported elsewhere.[16]

According to the literature, a loose apatite layer was apparent after 3 days of soaking and after 7 days, a dense apatite layer, composed of apatite particles with an obvious crystalline morphology was formed on the surface of BG microspheres.[9] After 7 days, a significant number of calcium phosphate (CaP) nodules developed on the surface of the PLA/BG composite microspheres. These nodules emerged

https://doi.org/10.1021/acsmaterialsau.3c00048
ACS Mater. Au 2023, 3, 646−658

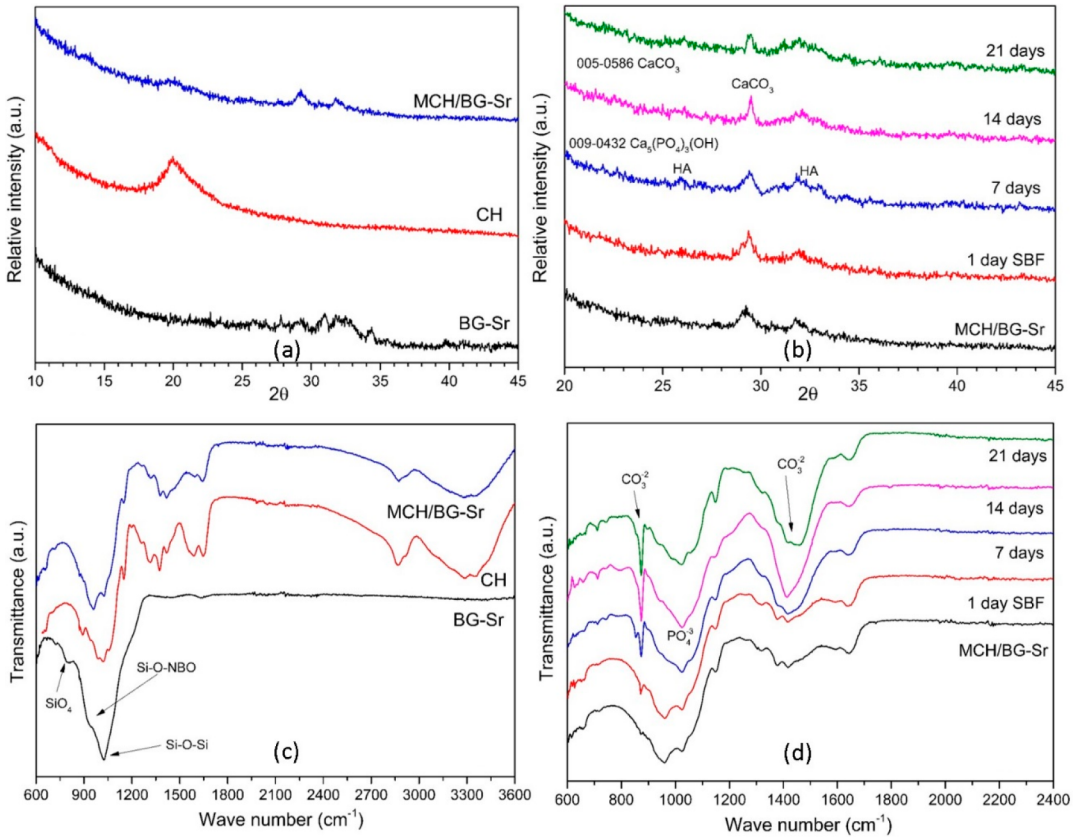

Figure 5. (a, b) XRD patterns and (c, d) FTIR spectra of BG 58S-Sr and chitosan (CH) and biocomposite macrospheres (MCH/BG-Sr) produced by the ionotropic gelation technique, before and after soaking in SBF for different testing times.

either from the pores or near the openings that formed due to solvent evaporation.[14] It was proposed that the release of silicate ions from bioactive glasses led to their adsorption onto the surface of the organic polymer substrate, thereby initiating apatite nucleation on the polymer surface.[38] In the case of CH/BG composite microspheres, the presence of a biologically active hydroxycarbonate apatite (HCA) layer on their surfaces was observed. The biocomposite based on bioactive glass and CH polymer presented an excellent ability to form an apatite-like layer on its surface.[16] The association of CH with BG improved the formation and crystallization of the hydroxyapatite layer. The porous structure of the BG/CH composite microspheres produced by the freeze-drying method should be responsible for the formation of a dense apatite layer. Because of the porosity, the ionic exchanges between the microspheres and the SBF occurred easily, thus improving their bioactivity.[16] The lack of porosity in MCH/BG-Sr (Table 1) may explain the lower bioactivity verified for this composite.

According to the literature,[9] BG microspheres with 1 mm in diameter, uniform size distribution, a loose microstructure containing numerous micropores on their surface and the interior were also produced by the method of combining alginate cross-linking $CaCl_2$ with heat treatment. The Si containing ionic products from the BG microspheres stimulated cell proliferation.

BG/PLA microspheres (100−200 μm) also present submicrometer-size pores on their surface as revealed by SEM analyses. The surface of microspheres was fully covered by carbonated calcium hydroxyapatite after 2 weeks of SBF immersion. On the other hand, PLA microspheres showed no evidence of calcium phosphate deposition. This can indicate that Si released from BG is involved in the formation of the Ca−P layer.[14]

In opposition to the results obtained in this work, the BG/CH biocomposite had a microsphere porous structure with formation of a carbonated hydroxyapatite layer on the surfaces after 3 days of SBF immersion. The addition of CH in the glass matrix also enhanced the cell proliferation of about 5% at 6 days after culturing.[16]

The bioactivity mechanism can be elucidated by a series of chemical reactions that take place when the bioglass is immersed in SBF. Initially, there is a rapid exchange of protons (H_3O^+) from the physiological solution with modifier cations present in the bioglass, leading to the formation of silanol bonds (SiOH) on the surface. This process is accompanied by the breaking of the Si−O−Si bridging linkage and subsequent generation of surface silanol groups due to an increase in pH. Subsequently, the surface silanols undergo condensation and repolymerization, resulting in the formation of a SiO_2-rich surface layer. Finally, there is the formation of an amorphous calcium phosphate layer, facilitated by the migration of Ca_2^+ and PO_4^{3-} ions from both the material and the surrounding medium toward the surface.[16,39,40]

The pH change of the SBF solution after contact with the macrospheres is shown in Figure 7. The initial pH of SBF was 7.4. MBG-Sr macrospheres reached the highest pH values as a function of time (~9.5) due to their dissolution process and the direct contact with SBF. The MCH/BG-Sr composites reached intermediate values (~9.0) because the presence of CH retarded the dissolution of bioglass while the lowest pH values were obtained for MPLA/BG-Sr composites (~8.0) due to the degradation of PLA to decrease the pH of the medium.

https://doi.org/10.1021/acsmaterialsau.3c00048
ACS Mater. Au 2023, 3, 646−658

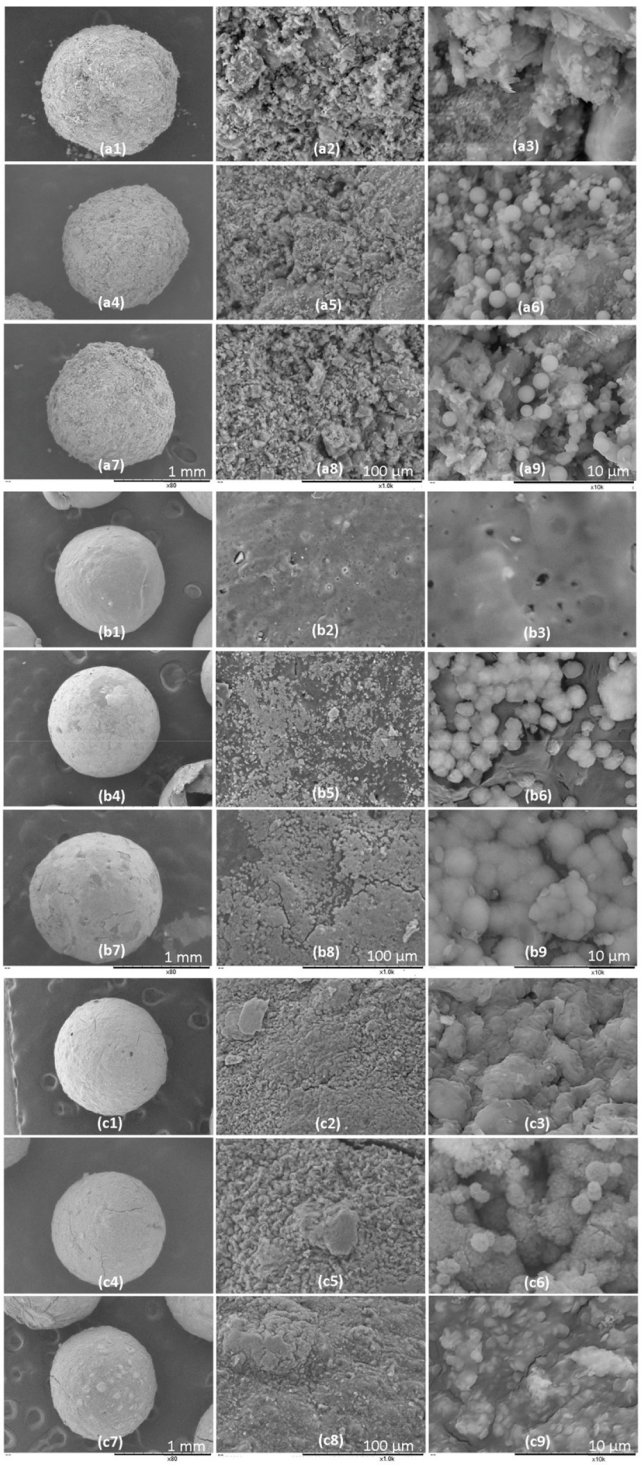

Figure 6. SEM images of biocomposite macrospheres: (a) BG-Sr, (b) PLA/BG-Sr, and (c) CH/BG-Sr (1−3) before, (4−6) after 7 days, and (7−9) after 14 days of soaking in SBF solution (×80, 1000, and 10 000).

PLA is a bioresorbable polymer composed of constitutive repeating units with −O−CHCH$_3$−CO− and present acidic degradation products. Its degradation is essentially due to chemical hydrolysis, governed by the accessibility of water to the ester bonds of the main chain. The carboxylic and hydroxyl groups resulting from hydrolysis generate an acidic microenvironment within the polymeric matrix.[14] According to the literature,[41] the pH value reached is critical for the formation

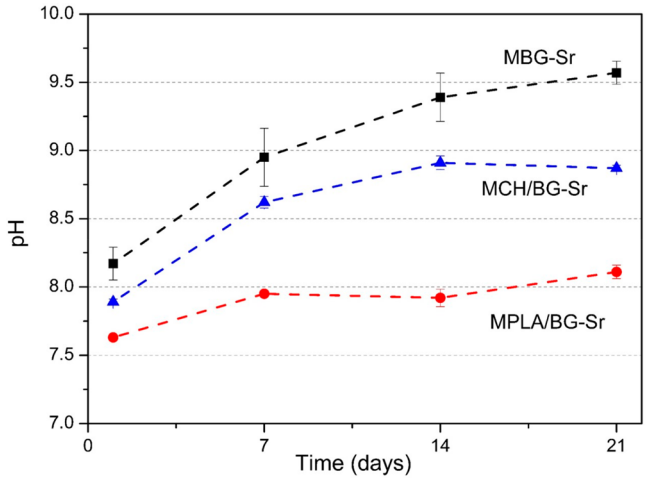

Figure 7. pH measurements of SBF solution after contact with samples of BG 58S-Sr macrospheres (MBG-Sr) and biocomposite macrospheres with PLA (MPLA/BG-Sr) and chitosan (MCH/BG-Sr).

of hydroxyapatite and the alkaline region (7.5−8.0) is ideal for its precipitation and crystallization. The pH increase above this ideal region probably can explain the observation of amorphous CaP precipitation.

3.3. Cytotoxicity Screening of BG-Sr Macrospheres

The results of the relative cell viability of SaOS-2 cells in the presence of a different concentration of extract obtained by contact with BG powders and macrospheres are shown in Figure 8. The compositions, except for those prepared with CH, showed cytotoxicity at the highest concentration of extract (100 mg/mL). The study has shown the absence deleterious cytotoxicity over osteoblast-like cells (SaOS-2 cells) when contact with leachable of BG/CH composite microspheres.[16]

The MCH/BG-Sr composites presented statistical differences of cell viability when compared to the control only for a higher concentration of extract (100 mg/mL). For MBG-Sr macrospheres, this occurred until concentration of 25 mg/mL, and for MPLA/BG-Sr all concentrations of extract resulted in statistical differences compared to control.

In the case of compositions prepared with PLA, significant cell death occurred even when the most diluted extracts (25 mg/mL) were tested. In this case, increasing the pH of the medium due to the degradation of the bioactive glass is probably accelerating the degradation of PLA making the medium acidic, which can promote cell toxicity.[14] PLA degradation rate might be accelerated in the alkaline environment resulting from the reactions of bioactive glass with the surrounding fluid.[14,42] According to the literature, the incorporation of BG powders into PLGA polymers significantly enhanced the degradation rate of PLGA.[43] Due to this, glass powders used in the preparation of MPLA/BG-Sr were previously immersed in simulated physiological fluid for 3 days before use.[14] Thus, when degradation occurred, the glass powders reacted with body fluids and created a local alkaline environment that neutralized the acidic pH of polymeric degradation. This may explain why the pH reached was lower for the PLA/BG macrospheres as compared to others (Figure 7). Moreover, the preformed HA surface layer on the macrospheres by immersion in SBF serves to protect PLA from degradation.[14]

https://doi.org/10.1021/acsmaterialsau.3c00048
ACS Mater. Au 2023, 3, 646−658

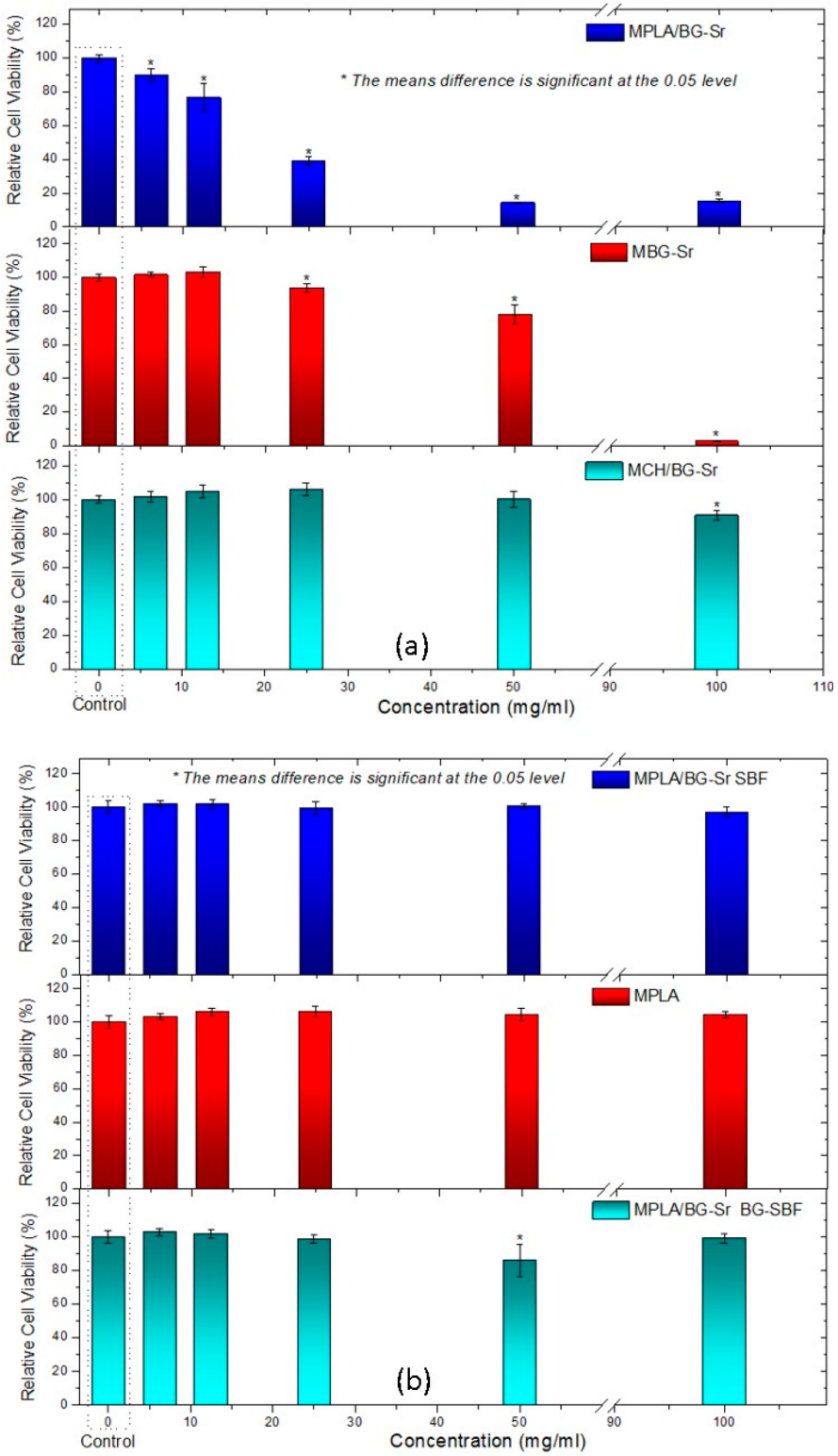

Figure 8. Relative cell viability of SaOS-2 cells after contacting with (a) different concentrations of extract obtained by contact with macrospheres (MBG-Sr) and biocomposite macrospheres (MPLA/BG-Sr, MCH/BG-Sr), and (b) with PLA/BG-Sr macrospheres treated in SBF or macrospheres produced using BG after being treated in SBF as compared to microspheres without BG-Sr (MPLA) for 48 h.

Based on that, in this work, the cell viability was also evaluated for MPLA/BG-Sr, which was soaked in SBF before the assays or using macrospheres prepared with BG-Sr powder previously treated in SBF. For both cases, the viability obtained was high even for the highest concentration of the extract. In addition, the viability was also high in all extract concentrations when only biocomposite macrospheres produced in the absence of BG-Sr were evaluated (MPLA). This confirmed that the observed effects on SaOS-2 cells viability may be associated with the influence of BG on the degradation of PLA. As recently discussed in the literature, the use of PLA for the fabrication of microspheres in bone tissue engineering presents

https://doi.org/10.1021/acsmaterialsau.3c00048
ACS Mater. Au 2023, 3, 646−658

as disadvantages byproducts due to acidic degradation limiting their application while the use of CH presents allergy risk and low cellular interaction.[4]

The treatment with simulated body fluid resulted in an apatite coating deposited on the surface of PLA microspheres promoting their osteoconductivity and osseointegration with the host tissues. Cells were proliferating better on PLA microspheres that were mineralized for a longer time, which is an indication that biomimetic mineralization may effectively promote interaction between the cells and materials.[44]

In addition to material degradation, the surface properties of microspheres such as roughness also can influence adhesion and, consequently, cells viability. High percentage of osteoblasts cells preferentially bind to rough surfaces instead of polished ones.[45] MPLA/BG-Sr surfaces were smoother than those of BG-Sr and MCH/BG-Sr composites before SBF treatment. Apatite precipitation on the MPLA/BG-Sr surface promoted a roughness increase.

In brief, biocomposite macrospheres including different polymers containing bioactive ceramics and Sr that can increase their biological properties were fabricated. We expect that this prospective work can contribute to increasing the application of biocomposite macrospheres in bone tissue repair applications. PLA/BG-Sr biocomposites presented a great potential for application in bone repair and reconstruction by combining the bioactive factors with the bioresorbable property and low density of the polymer. In addition it is expected that the effect of Sr incorporation can be proved in the next *in vitro* and *in vivo* assays that will be performed for the compositions studied in the present work.[46,47]

Studies on microsphere application in the bone tissue engineering field remain few. Currently, only ceramic-based microsphere products are used in orthopedics and dentistry. The clinical efficacy of polymer-based microspheres in orthopedics remains difficult to assess because of the lack of long-term clinical data.[4]

4. CONCLUSIONS

In this work, strontium-bioactive glass macrospheres were produced by encapsulation techniques using sodium alginate, poly(lactic acid) (PLA), and chitosan (CH) as the encapsulating material. The MPLA/BG-Sr macrospheres have a larger size distribution and more porosity compared to others, MBG-Sr, and MCH/BG-Sr. Loose apatite particles are observed on the surface of macrospheres prepared with alginate and CH. On the other hand, a dense apatite layer is formed on the MPLA/BG-Sr macrospheres. These composites result in an ideal pH value for hydroxyapatite precipitation and crystallization. In addition, the more porous structure of these composites observed by micro-CT compared to MCH/BG-Sr should be responsible for the formation of a dense apatite layer. The MPLA/BG-Sr macrospheres also present a cytotoxic effect over osteoblast cells because the PLA degradation rate is accelerated in the alkaline environment resulting from the reactions of bioactive glass with the surrounding fluid, which may be responsible for the observed decrease in cells viability. Then, the bioactive glass powder previously treated in SBF must be incorporated into the PLA matrix to avoid its accelerated degradation. Treatment of MPLA/BG-Sr by immersion in SBF to precipitate a hydroxyapatite surface layer can also be realized to protect PLA from degradation and thus help enhancing the biocomposites cytocompatibility. Based on our findings, the PLA/BG-Sr biocomposites have great potential for application in bone repair and reconstruction combining the bioactive factors of bioactive glasses and strontium with the bioresorbable property and low density of the polymer.

AUTHOR INFORMATION

Corresponding Author

Ivone Regina de Oliveira − *Institute for Research and Development, University of Vale do Paraíba, São Paulo 12244-000, Brazil*; Phone: +55(12-3947-1100); Email: ivoneregina.oliveira@gmail.com; Fax: +55(12-3947-1120)

Authors

Isabela dos Santos Gonçalves − *Institute for Research and Development, University of Vale do Paraíba, São Paulo 12244-000, Brazil*

Kennedy Wallace dos Santos − *Institute for Research and Development, University of Vale do Paraíba, São Paulo 12244-000, Brazil; Selaz − Industry and Commercialization of Biomechanical Devices, São Paulo 12244-000, Brazil*

Maria Carmo Lança − *CENIMAT|i3N, Department of Materials Science, NOVA School of Science and Technology, NOVA University Lisbon, Caparica 2829-516, Portugal*

Tânia Vieira − *Tissue Engineering Laboratory, NOVA School of Science and Technology, NOVA University Lisbon, Caparica 2829-516, Portugal*

Jorge Carvalho Silva − *Tissue Engineering Laboratory, NOVA School of Science and Technology, NOVA University Lisbon, Caparica 2829-516, Portugal;* orcid.org/0000-0001-9959-4272

Ibrahim Fatih Cengiz − *3B's Research Group, I3Bs—Research Institute on Biomaterials, Biodegradables and Biomimetics, University of Minho, Headquarters of the European Institute of Excellence on Tissue Engineering and Regenerative Medicine, AvePark, Parque de Ciência e Tecnologia, Zona Industrial da Gandra, Barco, Guimarães 4805-017, Portugal; ICVS/3B's—PT Government Associate Laboratory, Braga 4710-057, Portugal;* orcid.org/0000-0003-0886-632X

Rui Luís Reis − *3B's Research Group, I3Bs—Research Institute on Biomaterials, Biodegradables and Biomimetics, University of Minho, Headquarters of the European Institute of Excellence on Tissue Engineering and Regenerative Medicine, AvePark, Parque de Ciência e Tecnologia, Zona Industrial da Gandra, Barco, Guimarães 4805-017, Portugal; ICVS/3B's—PT Government Associate Laboratory, Braga 4710-057, Portugal;* orcid.org/0000-0002-4295-6129

Joaquim Miguel Oliveira − *3B's Research Group, I3Bs—Research Institute on Biomaterials, Biodegradables and Biomimetics, University of Minho, Headquarters of the European Institute of Excellence on Tissue Engineering and Regenerative Medicine, AvePark, Parque de Ciência e Tecnologia, Zona Industrial da Gandra, Barco, Guimarães 4805-017, Portugal; ICVS/3B's—PT Government Associate Laboratory, Braga 4710-057, Portugal;* orcid.org/0000-0001-7052-8837

João Paulo Miranda Ribeiro Borges − *CENIMAT|i3N, Department of Materials Science, NOVA School of Science and Technology, NOVA University Lisbon, Caparica 2829-516, Portugal;* orcid.org/0000-0002-3996-6545

https://doi.org/10.1021/acsmaterialsau.3c00048
ACS Mater. Au 2023, 3, 646−658

Complete contact information is available at:
https://pubs.acs.org/10.1021/acsmaterialsau.3c00048

Notes

The authors declare no competing financial interest.

■ ACKNOWLEDGMENTS

This work was funded by grant #2019/15960-6, São Paulo Research Foundation in Brazil (FAPESP) and the Portuguese Foundation for Science and Technology (FCT), Reference UID/CTM/50025/2019 and FCT/Minister of Science, Technology and Higher Education in Portugal (MCTES) and by European Regional Development Fund (FEDER) funds through the COMPETE 2020 Program in the framework of ORAiDEA project (ref n° 39985 - AAC 31/SI/2017). The authors would also like to acknowledge Materials Research Center (CENIMAT) of the Associated Laboratory Institute of Nanostructures, Nanomodeling and Nanofabrication (i3N), NOVA University of LisbonCENIMAT|i3N and National Council for Scientific and Technological Development in Brazil CNPq (303149/2018-3). Ibrahim Fatih Cengiz acknowledges the FCT distinction attributed to him under the "Estímulo ao Emprego Científico" program (2021.01969.CEECIND). The authors thank the financial support provided under the projects: "HEALTH-UNORTE: Setting-up biobanks and regenerative medicine strategies to boost research in cardiovascular, musculoskeletal, neurological, oncological, immunological, and infectious diseases", reference NORTE-01-0145-FEDER-000039, funded by the Norte Portugal Regional Coordination and Development Commission (CCDR-N), under the NORTE2020 Program; Projects LA/P/0037/2020, UIDP/50025/2020, and UIDB/50025/2020 of the Associate Laboratory i3N financed by national funds from FCT.

■ REFERENCES

(1) Heitzmann, L. G.; Battisti, R.; Rodrigues, A. F.; Lestingi, J. V.; Cavazzana, C.; Queiroz, R. D. Postoperative chronic osteomyelitis in the long bones-current knowledge and management of the problem. *Revista Brasileira de Ortopedia* **2019**, *54*, 627−635.

(2) Kaur, G.; Pickrell, G.; Sriranganathan, N.; Kumar, V.; Homa, D. Review and the state of the art: sol-gel and melt quenched bioactive glasses for tissue engineering. *Journal of Biomedical Materials Research Part B: Applied Biomaterials* **2016**, *104* (6), 1248−1275.

(3) Dantas, T. S.; Lelis, É. R.; Naves, L. Z.; Fernandes-Neto, A. J. Materiais de enxerto ósseo e suas aplicações na odontologia [Bone graft materials and their applications in dentistry]. *Journal of Health Sciences* **2011**, *13* (2), 131−135.

(4) Cai, Z.; Jiang, H.; Lin, T.; Wang, C.; Ma, J.; Gao, R.; Jiang, Y.; Zhou, X. Microspheres in bone regeneration: Fabrication, properties and applications. *Materials Today Advances* **2022**, *16*, 100315.

(5) Greenwald, A. S.; Boden, S. D.; Goldberg, V. M.; Khan, Y.; Laurencin, C. T.; Rosier, R. N. Bone-graft substitutes: facts, fictions, and applications. *Jbjs* **2001**, *83* (2), 98−103.

(6) Soares, M. V. R. *Biomateriais utilizados na prática odontológica: uma revisão de literatura*. Monografia-Curso de Odontologia da Universidade Estadual de Londrina, Londrina, 2015.

(7) Baino, F.; Hamzehlou, S.; Kargozar, S. Bioactive glasses: where are we and where are we going? *Journal of functional biomaterials* **2018**, *9* (1), 25.

(8) Jones, J. R.; Brauer, D. S.; Hupa, L.; Greenspan, D. C. Bioglass and bioactive glasses and their impact on healthcare. *International Journal of Applied Glass Science* **2016**, *7* (4), 423−434.

(9) Wu, C.; Zhang, Y.; Ke, X.; Xie, Y.; Zhu, H.; Crawford, R.; Xiao, Y. Bioactive mesopore-glass microspheres with controllable protein-delivery properties by biomimetic surface modification. *J. Biomed. Mater. Res., Part A* **2010**, *95* (2), 476−485.

(10) *In vivo evaluation of bioSphere bioactive bone graft putty: improved bone formation*. Synergy Biomedical, 2022. http://www.synergybiomedical.com/in-vivo-bone-healing.html (accessed 2023-05-23).

(11) Sarker, B.; Papageorgiou, D. G.; Silva, R.; Zehnder, T.; Gul-E-Noor, F.; Bertmer, M.; Kaschta, J.; Chrissafis, K.; Detsch, R.; Boccaccini, A. R. Fabrication of alginate-gelatin crosslinked hydrogel microcapsules and evaluation of the microstructure and physico-chemical properties. *J. Mater. Chem. B* **2014**, *2* (11), 1470−1482.

(12) de Araújo Etchepare, M.; Rodrigues, L. Z.; Codevilla, C. F.; de Menezes, C. R. Microencapsulação de compostos bioativos pelo método de extrusão [Microencapsulation of bioactive compounds by the extrusion method]. *Ciência e Natura* **2015**, *37* (5), 97−105.

(13) Zhu, T.; Ren, H.; Li, A.; Liu, B.; Cui, C.; Dong, Y.; Tian, Y.; Qiu, D. Novel bioactive glass based injectable bone cement with improved osteoinductivity and its in vivo evaluation. *Sci. Rep.* **2017**, *7* (1), 3622.

(14) Qiu, Q. Q.; Ducheyne, P.; Ayyaswamy, P. S. New bioactive, degradable composite microspheres as tissue engineering substrates. *J. Biomed. Mater. Res.* **2000**, *52* (1), 66−76.

(15) Rottensteiner-Brandl, U.; Detsch, R.; Sarker, B.; Lingens, L.; Köhn, K.; Kneser, U.; Bosserhoff, A. K.; Horch, R. E.; Boccaccini, A. R.; Arkudas, A. Encapsulation of rat bone marrow derived mesenchymal stem cells in alginate dialdehyde/gelatin microbeads with and without nanoscaled bioactive glass for in vivo bone tissue engineering. *Materials* **2018**, *11* (10), 1880.

(16) Bui, X.-V.; Oudadesse, H.; Le Gal, Y.; Mostafa, A.; Cathelineau, G. Microspheres of chitosan-bioactive glass for application in orthopedic surgery. In vitro experiment. In *Recent Researches in Modern Medicine*; WSEAS Press, 2011; pp 359−367.

(17) Oliveira, I.; Barbosa, A.; Grancianinov, K.; Origo, F.; Dos Santos, K.; Leite, P.; Raniero, L.; Pandolfelli, V. Surface properties of calcium aluminate cement blends for bone repair applications. *Ceram. Int.* **2020**, *46* (9), 14241−14251.

(18) Jiménez, M.; Abradelo, C.; San Román, J.; Rojo, L. Bibliographic review on the state of the art of strontium and zinc based regenerative therapies. Recent developments and clinical applications. *J. Mater. Chem. B* **2019**, *7* (12), 1974−1985.

(19) Ereiba, K.; Abd Raboh, A.; Mostafa, A. Characterization of some bioactive glasses based on SiO 2-CaO-P 2 O 5-SrO quaternary system prepared by sol-gel method. *Nat. Sci.* **2014**, *12* (5), 97−105.

(20) Querido, W.; Rossi, A. L.; Farina, M. The effects of strontium on bone mineral: A review on current knowledge and microanalytical approaches. *Micron* **2016**, *80*, 122−134.

(21) Oliveira, I.; Barbosa, A.; Santos, K.; Lança, M.; Lima, M.; Vieira, T.; Silva, J.; Borges, J. Properties of strontium-containing BG 58S produced by alkali-mediated sol-gel process. *Ceram. Int.* **2022**, *48* (8), 11456−11465.

(22) Liu, X.; Yu, W.; Zhang, Y.; Xue, W.; Yu, W.; Xiong, Y.; Ma, X.; Chen, Y.; Yuan, Q. Characterization of structure and diffusion behaviour of Ca-alginate beads prepared with external or internal calcium sources. *J. Microencapsulation* **2002**, *19* (6), 775−782.

(23) Ching, S. H.; Bansal, N.; Bhandari, B. Alginate gel particles-A review of production techniques and physical properties. *Critical reviews in food science and nutrition* **2017**, *57* (6), 1133−1152.

(24) Sun, J.; Tan, H. Alginate-based biomaterials for regenerative medicine applications. *Materials* **2013**, *6* (4), 1285−1309.

(25) Heng, P.; Chan, L.; Wong, T. Formation of alginate microspheres produced using emulsification technique. *J. Microencapsulation* **2003**, *20* (3), 401−413.

(26) Dash, M.; Chiellini, F.; Ottenbrite, R.; Chiellini, E. Progress in Polymer Science. Chitosan-A versatile semi-synthetic polymer in biomedical applications. *Biomaterials* **2011**, *36* (8), 981−1014.

(27) Cengiz, I. F.; Oliveira, J. M.; Reis, R. L. Micro-computed tomography characterization of tissue engineering scaffolds: effects of pixel size and rotation step. *J. Mater. Sci.: Mater. Med.* **2017**, *28*, 1−11.

(28) Cengiz, I. F.; Oliveira, J. M.; Reis, R. L. Micro-CT-a digital 3D microstructural voyage into scaffolds: a systematic review of the reported methods and results. *Biomaterials research* **2018**, *22*, 1−11.
(29) Cengiz, I. F.; Maia, F. R.; da Silva Morais, A.; Silva-Correia, J.; Pereira, H.; Canadas, R. F.; Espregueira-Mendes, J.; Kwon, I. K.; Reis, R. L.; Oliveira, J. M. Entrapped in cage (EiC) scaffolds of 3D-printed polycaprolactone and porous silk fibroin for meniscus tissue engineering. *Biofabrication* **2020**, *12* (2), 025028.
(30) Cengiz, I. F.; Pereira, H.; Espregueira-Mendes, J.; Kwon, I. K.; Reis, R. L.; Oliveira, J. M. Suturable regenerated silk fibroin scaffold reinforced with 3D-printed polycaprolactone mesh: biomechanical performance and subcutaneous implantation. *J. Mater. Sci.: Mater. Med.* **2019**, *30*, 1−17.
(31) Sepulveda, P.; Jones, J.; Hench, L. In vitro dissolution of melt-derived 45S5 and sol-gel derived 58S bioactive glasses. *Journal of Biomedical Materials Research: An Official Journal of The Society for Biomaterials, The Japanese Society for Biomaterials, and The Australian Society for Biomaterials and the Korean Society for Biomaterials* **2002**, *61* (2), 301−311.
(32) Nariyal, R.; Kothari, P.; Bisht, B. FTIR measurements of SiO 2 glass prepared by sol-gel technique. *Chemical Science Transactions* **2014**, *3* (3), 1064−1066.
(33) Bui, X. V.; Dang, T. H. Bioactive glass 58S prepared using an innovation sol-gel process. *Processing and application of ceramics* **2019**, *13* (1), 98−103.
(34) Kalampounias, A. G. IR and Raman spectroscopic studies of sol-gel derived alkaline-earth silicate glasses. *Bulletin of Materials Science* **2011**, *34*, 299−303.
(35) Maçon, A. L.; Lee, S.; Poologasundarampillai, G.; Kasuga, T.; Jones, J. R. Synthesis and dissolution behaviour of CaO/SrO-containing sol-gel-derived 58S glasses. *J. Mater. Sci.* **2017**, *52*, 8858−8870.
(36) Luz, G. M.; Mano, J. F. Preparation and characterization of bioactive glass nanoparticles prepared by sol-gel for biomedical applications. *Nanotechnology* **2011**, *22* (49), 494014.
(37) Siqueira, R. L.; Zanotto, E. D. The influence of phosphorus precursors on the synthesis and bioactivity of SiO 2-CaO-P 2 O 5 sol-gel glasses and glass-ceramics. *J. Mater. Sci.: Mater. Med.* **2013**, *24*, 365−379.
(38) Xia, W.; Chang, J. Preparation and characterization of nano-bioactive-glasses (NBG) by a quick alkali-mediated sol-gel method. *Materials letters* **2007**, *61* (14−15), 3251−3253.
(39) Rezaei, Y.; Moztarzadeh, F.; Shahabi, S.; Tahriri, M. Synthesis, characterization, and in vitro bioactivity of sol-gel-derived SiO2-CaO-P2O5-MgO-SrO bioactive glass. *Synthesis and Reactivity in Inorganic, Metal-Organic, and Nano-Metal Chemistry* **2014**, *44* (5), 692−701.
(40) Tanahashi, M.; Yao, T.; Kokubo, T.; Minoda, M.; Miyamoto, T.; Nakamura, T.; Yamamuro, T. Apatite coated on organic polymers by biomimetic process: improvement in its adhesion to substrate by NaOH treatment. *Journal of Applied Biomaterials* **1994**, *5* (4), 339−347.
(41) De Aza, P.; Guitian, F.; Merlos, A.; Lora-Tamayo, E.; De Aza, S. Bioceramics—simulated body fluid interfaces: pH and its influence of hydroxyapatite formation. *J. Mater. Sci.: Mater. Med.* **1996**, *7*, 399−402.
(42) Navarro, M.; Ginebra, M.; Planell, J.; Barrias, C.; Barbosa, M. In vitro degradation behavior of a novel bioresorbable composite material based on PLA and a soluble CaP glass. *Acta Biomaterialia* **2005**, *1* (4), 411−419.
(43) Wu, C.; Ramaswamy, Y.; Zhu, Y.; Zheng, R.; Appleyard, R.; Howard, A.; Zreiqat, H. The effect of mesoporous bioactive glass on the physiochemical, biological and drug-release properties of poly (DL-lactide-co-glycolide) films. *Biomaterials* **2009**, *30* (12), 2199−2208.
(44) Shi, X.; Jiang, J.; Sun, L.; Gan, Z. Hydrolysis and biomineralization of porous PLA microspheres and their influence on cell growth. *Colloids Surf., B* **2011**, *85* (1), 73−80.
(45) Lim, Y. J.; Oshida, Y.; Andres, C. J.; Barco, M. T. Surface characterizations of variously treated titanium materials. *Int. J. Oral Maxillofa. Implants* **2001**, *16* (3), 333−342.
(46) Chen, Y.; Liu, Z.; Jiang, T.; Zou, X.; Lei, L.; Yan, W.; Yang, J.; Li, B. Strontium-substituted biphasic calcium phosphate microspheres promoted degradation performance and enhanced bone regeneration. *J. Biomed. Mater. Res., Part A* **2020**, *108* (4), 895−905.
(47) Kargozar, S.; Montazerian, M.; Fiume, E.; Baino, F. Multiple and promising applications of strontium (Sr)-containing bioactive glasses in bone tissue engineering. *Frontiers in bioengineering and biotechnology* **2019**, *7*, 161.

https://doi.org/10.1021/acsmaterialsau.3c00048
ACS Mater. Au 2023, 3, 646−658